

Interpreting Galilean Invariant Vector Field Analysis via Extended Robustness *

Bei Wang, Roxana Bujack, Paul Rosen, Primoz Skraba, Harsh Bhatia, Hans Hagen

Abstract The topological notion of robustness introduces mathematically rigorous approaches to interpret vector field data. Robustness quantifies the structural stability of critical points with respect to perturbations and has been shown to be useful for increasing the visual interpretability of vector fields. However, critical points, which are essential components of vector field topology, are defined with respect to a chosen frame of reference. The classical definition of robustness, therefore, depends also on the chosen frame of reference. We define a new Galilean invariant robustness framework that enables the simultaneous visualization of robust critical points across the dominating reference frames in different regions of the data. We also demonstrate a strong connection between such a robustness-based framework with the one recently proposed by Bujack et al., which is based on the determinant of the Jacobian. Our results include notable observations regarding the definition of stable features within the vector field data.

Bei Wang
University of Utah, e-mail: beiwang@sci.utah.edu

Roxana Bujack
Los Alamos National Laboratory, e-mail: bujack@lanl.gov

Paul Rosen
University of South Florida, e-mail: prosen@usf.edu

Primoz Skraba
Jozef Stefan Institute, e-mail: primoz.skraba@ijs.si

Harsh Bhatia
Lawrence Livermore National Laboratory, e-mail: hbhatia@llnl.gov

Hans Hagen
Technical University Kaiserslautern, e-mail: hagen@informatik.uni-kl.de

* This work was partially supported by NSF IIS-1513616, National Research Agency ARRS Project TopRep N1-0058.

1 Introduction

Motivation. Understanding vector fields is integral to many scientific applications ranging from combustion to global oceanic eddy simulations. Critical points of a vector field (i.e., zeros of the field) are essential features of the data and play an important role in describing and interpreting the flow behavior. However, vector field analysis based on critical points suffers a major drawback: the interpretation of critical points depends upon the chosen frame of reference. Just like the velocity field itself, they are not Galilean invariant. Fig. 1 highlights this limitation, where the critical points in a simulated flow (the von Kármán vortex street) are visible only when the velocity of the incoming flow is subtracted.

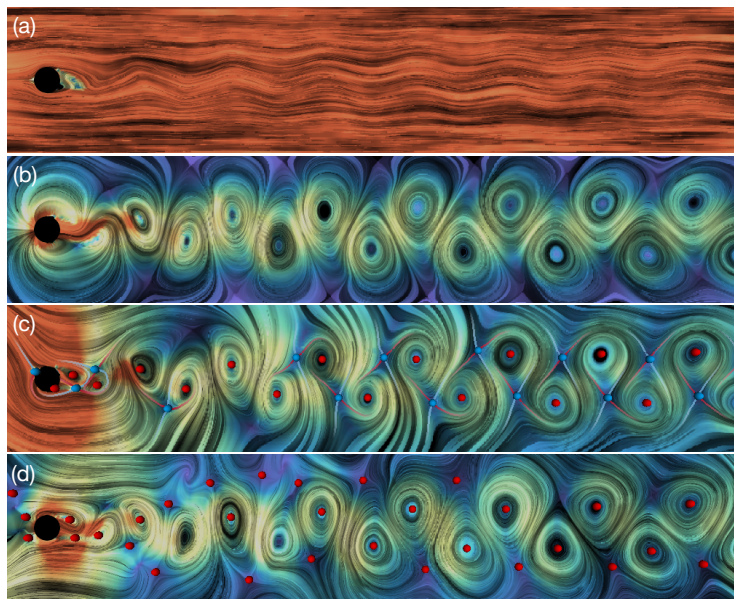


Fig. 1 Visualization of the flow behind a cylinder without (a) and with (b) the background flow removed, where the colormap encodes the speed of the flow. For comparison, (c) shows the corresponding Galilean invariant vector field introduced by Bujack et al. which is constructed from the extrema of the determinant of the Jacobian. The Galilean invariant critical points are marked with red nodes for vortices/sources/sinks and with blue nodes for saddles. Image courtesy of Bujack et al. [2]. (d) Galilean invariant vector field constructed from the extended robustness. The local maxima of the extended robustness field are marked with red nodes.

The extraction of *meaningful* features in the data therefore depends on a *good* choice of a reference frame. Oftentimes, there exists no single frame of reference that enables simultaneous visualization of *all* relevant features. For example, it is not possible to find one single frame that simultaneously shows the von Kármán vortex street from Fig. 1(b) and the first vortex formed directly behind the obstacle in Fig. 1(a). To overcome such a drawback, a framework recently introduced by Bujack

et al. [2] considers every point as critical and locally adjusts the frame of reference to enable simultaneous visualization of dominating frames that highlight features of interest. Such a framework selects a subset of critical points based on Galilean invariant criteria and visualizes their frame of reference in their local neighborhood. Galilean invariance refers to the principle that Newton's laws hold in all frames moving at a uniform relative velocity. Thus, a Galilean invariant property is one that does not change when observed in different frames with uniform motion relative to each other. The extrema of the determinant of the Jacobian are particular examples of Galilean invariant critical points [2], and they simultaneously capture all relevant features in the data, as illustrated in Fig. 1(c). The intuition is that the determinant of the Jacobian determines the type of critical point, and since the Jacobian is Galilean invariant, its extrema (with a magnitude away from zero) correspond to *stable* critical point locations where small perturbations in the field do not change their types. Such Galilean invariant critical points, in general, do not overlap with the classical zeros of the vector fields; however, each has a frame of reference in which it is a zero of the field. Such a perspective is useful in revealing features beyond those obtainable with a single frame of reference (e.g., Fig. 1(c)).

The topological notion of robustness, on the other hand, considers the *stability* of critical points with respect to perturbations. Robustness, a concept closely related to *topological persistence* [10], quantifies the stability of critical points, and, therefore, assesses their significance with respect to perturbations to the field. Intuitively, the robustness of a critical point is the minimum amount of perturbation necessary to cancel it within a local neighborhood. Robustness, therefore, helps in interpreting a vector field in terms of its structural stability. Several studies have shown it to be useful for increasing the visual interpretability of vector fields [29] in terms of feature extraction, tracking [25], and simplification [24, 26, 27].

Contributions. In this paper, we present new and intriguing observations connecting the Jacobian based and robustness based notions in quantifying stable critical points in vector fields. In particular, we address the following questions: *Can we interpret Galilean invariant vector field analysis based on the determinant of the Jacobian via the notion of robustness? What are the relations between these two seemingly different notions?* Our contributions are:

- We extend the definition of robustness by considering every point as a critical point and introduce the notion of the *extended robustness* field by assigning each point in the domain its robustness when it is made critical with a proper frame of reference.
- We prove that the extended robustness satisfies the criterion of Galilean invariance, where the local maxima of the extended robustness field are the Galilean invariant critical points.
- We prove, theoretically, that the determinant of the Jacobian is a lower bound for the extended robustness at the same point.
- We demonstrate, visually, that the extended robustness helps to interpret the Jacobian-based Galilean invariant vector field analysis, in particular, that the extrema of the determinant of the Jacobian coincide with the local maxima of the extended robustness (Fig. 1(c)-(d)).

2 Related Work

Vector field analysis and reference frames. The analysis of vector fields depends upon the chosen frame of reference [20, 21, 22], as the observed vector field changes with changes in frames. In particular, for any one given point, it is always possible to create a frame of reference where this point becomes critical. Therefore, it is important to carefully choose a physically meaningful frame for analysis. In this regard, uniformly moving frames are of particular importance as they preserve many properties of interest, thus providing a *Galilean invariant* analysis.

Because of the physical importance of a feature descriptor to be independent from a Galilean change of frame of reference, many popular vector field feature detectors are Galilean invariant. In particular, a number of vortex detection techniques, such as the λ_2 - [18], Q - [17], and Δ - [8] criterion, compute the Jacobian of the field, which, being a spatial derivative, discards uniform motion.

Simpler solutions to guarantee Galilean invariance in vector field analysis involve subtracting the mean vector to highlight the fluctuations in the field. In recent literature, more advanced techniques have been presented to derive vectors for subtraction to determine an expressive frame of reference, e.g., from the Helmholtz-Hodge decomposition [1, 30] or the boundary-induced flow [9]. In general, Galilean invariant frames have been employed extensively for vector field analysis [2, 7, 8, 19, 23].

Nevertheless, since Galilean invariance is limited to compensating for uniform motion, there exist techniques to perform the analysis in more sophisticated frames. For example, Haller [15] extracted vortices using time-dependent translations and time-dependent rotations; Günther et al. [14] described computation of vortices in rotational frames; Fuchs et al. [13] used time-varying frames built upon the notion of “unsteadiness”; and Bhatia et al. [1] proposed using new frames to represent harmonic background flows.

In this work, we consider Galilean invariance to be the key property for defining robustness for critical points across reference frames and extend the framework by Bujack et al. [2].

Robustness. The topological notion of robustness is closely related to the topological persistence [10]. Unlike persistence, which is used extensively for the analysis and visualization of scalar field data, robustness, first introduced by Edelsbrunner et al. [11], can be employed for vector field data [6, 12]. Recent work by Wang et al. [29] assigned robustness to critical points in both stationary and time-varying vector fields and obtained a hierarchical structural description of the data. Such a hierarchical description implies simplification strategies that perform critical point cancellations in both 2D [26, 27] and 3D [24]. The robustness framework also gives a fresh interpretation of the notion of feature tracking, in particular, critical point tracking, where robust critical points could provably be tracked more easily and more accurately in the time-varying setting [25].

Since robustness of critical points is not invariant to reference frames, in our work, we aim to define a new robustness framework that addresses such a challenge

and enables the simultaneous visualization of robustness across local, dominating reference frames.

3 Technical Background

We revisit some technical background before describing our results, namely, the notions of Galilean invariance, reference frame adjustment, Jacobian-based Galilean invariant vector fields, and robustness.

Galilean invariance. Let $v : \mathbb{R}^2 \rightarrow \mathbb{R}^2$ denote a 2D vector field describing the instantaneous velocity of a flow. A *Galilean transformation* of a point $x \in \mathbb{R}^2$ is the composition of a translation $b : \mathbb{R} \rightarrow \mathbb{R}^2$ with $\dot{b} = \text{const}$, and a rigid body rotation $A \in SO(2)$ [2]. A point whose position in the original frame is x , then has the coordinate in the transformed frame [28] as

$$x' = Ax + b. \quad (1)$$

A vector field $v(x)$ is *Galilean invariant* (GI) if it transforms under a *Galilean transformation*, according to the rule $v'(x') = Av(x)$ [28]. Similarly, a scalar field $s(x)$ and a matrix field $M(x)$ are called GI if $s'(x') = s(x)$ and $M'(x') = AM(x)A^{-1}$, respectively.

Reference frame adjustment. Every point in a vector field can be transformed into a critical point by the addition of a constant vector. For a vector field $v : \mathbb{R}^2 \rightarrow \mathbb{R}^2$ and a point $x_0 \in \mathbb{R}^2$, we define the associated vector field $v_{x_0} : \mathbb{R}^2 \rightarrow \mathbb{R}^2$ with its frame of reference based on x_0 by

$$v_{x_0}(x) := v(x) - v(x_0). \quad (2)$$

Such a vector field v_{x_0} has a permanent critical point at x_0 , because $v_{x_0}(x_0) = v(x_0) - v(x_0) = 0$. For a given position $x_0 \in \mathbb{R}^2$, the vector field v_{x_0} is GI, because from $v'(x') = dx'/dt \stackrel{(1)}{=} d(Ax + b)/dt = Av(x) + \dot{b}$ follows $v'_{x'_0}(x') \stackrel{(2)}{=} v'(x') - v'(x'_0) = Av(x) + \dot{b} - Av(x_0) - \dot{b} = A(v(x) - v(x_0)) \stackrel{(2)}{=} Av_{x_0}(x)$.

Jacobian-based Galilean invariant vector fields. Recall $v : \mathbb{R}^2 \rightarrow \mathbb{R}^2$ is a 2D vector field, where $v(x) = \dot{x} = dx/dt = (v_1(x), v_2(x))^T$. Let J denote the Jacobian of a velocity field,

$$J = \nabla v(x) = \begin{pmatrix} \partial v_1(x)/\partial x_1 & \partial v_1(x)/\partial x_2 \\ \partial v_2(x)/\partial x_1 & \partial v_2(x)/\partial x_2 \end{pmatrix}.$$

The determinant of the Jacobian, $\det(J)$, is shown to be a GI scalar field [2], that is, $\det J'(x') = \det J(x)$. Such a determinant can be used to categorize first-order critical points, that is, a negative determinant corresponds to a saddle, whereas a positive determinant corresponds to a source, a sink, or a vortex.

A point $(x_0) \in \mathbb{R}^2$ is a Jacobian-based *Galilean invariant critical point* (GICP) of a vector field $v : \mathbb{R}^2 \rightarrow \mathbb{R}^2$ if it is a critical point of the determinant of the Jacobian, i.e., $\nabla \det(J) := \nabla \det(\nabla v(x_0)) = 0$ [2]. Bujack et al. [2] restrict this definition to the negative minima and the positive maxima of the determinant field. The former form saddles, whereas the latter form sources/sinks/vortices in the velocity field in some specific frame of reference. Each GICP comes with its own frame of reference in which it becomes a classical critical point.

To visualize the GICPs simultaneously, Bujack et al. [2] introduced the notion of *Galilean invariant vector field* (GIVF) that is applicable beyond Jacobian-based GICPs. The basic idea is to construct a derived vector field that locally assumes the inherent frames of references of each GICP. Such a derived vector field is constructed by subtracting a weighted average of the velocities of the GICPs, x_1, \dots, x_n , of the vector field v .

Formally, let $v : \mathbb{R}^2 \rightarrow \mathbb{R}^2$ be a vector field, $x_1, \dots, x_n \in \mathbb{R}^2$ a set of GICPs, and w_i the weights of a linear interpolation problem $\sum_{i=1}^n w_i(x)v(x_i)$ with weights $w_i : \mathbb{R}^2 \rightarrow \mathbb{R}$ (and a mapping $x \mapsto w_i(x)$) that are invariant under Galilean transformation, that is,

$$w_i'(x') = w_i(x),$$

and the weights add up to one, $\forall x \in \mathbb{R}^2 : \sum_{i=1}^n w_i(x) = 1$. Then, the GIVF $\bar{v} : \mathbb{R}^2 \rightarrow \mathbb{R}^2$ is defined by

$$\bar{v}(x) := v(x) - \sum_{i=1}^n w_i(x)v(x_i).$$

In this paper, we use inverse distance weighting with exponent 2. Most commonly used weights satisfy such a condition such as the ones from constant, barycentric, bilinear, and inverse distance interpolations [2].

Remark. Locally the transformation in defining a GIVF is a Galilean change of reference. However depending on the chosen interpolation scheme, the points between the GICPs are transformed by a mixture of the transformations of their neighbors. This mixture does not generally result in a Galilean transformation globally. As a result, the Jacobian of the GIVF and the original field are not identical.

Although the suggested method does not transform the field through a Galilean transformation itself, it does not contradict the fact that the GIVF defined above is invariant with respect to the Galilean transformation [2]. Such a transformed vector field is GI, because any vector field that differs from the original one through a Galilean transformation will result in the same GIVF, which means that the GIVF and the original field would generally not produce the same output. In a nutshell, the method is GI, but not idempotent.

Robustness. Let $f, h : \mathbb{R}^2 \rightarrow \mathbb{R}^2$ be two continuous 2D vector fields. We define the distance between the two mappings as $d(f, h) = \sup_{x \in \mathbb{R}^2} \|f(x) - h(x)\|_2$. The field h is an r -perturbation of f , if $d(f, h) \leq r$. Given $f : \mathbb{R}^2 \rightarrow \mathbb{R}^2$, the *robustness* of a critical point of f quantifies its stability with respect to perturbations of the vector fields [29]. Intuitively, if a critical point has a robustness value of r , then an

$(r + \delta)$ -perturbation h of f exists to eliminate x (via critical point cancellation); and any $(r - \delta)$ -perturbation is not enough to eliminate x .

Mathematically, the robustness of critical points in our setting arises from the well group theory [12]. Given a mapping $f : \mathbb{X} \rightarrow \mathbb{Y}$ between two manifolds and a point $a \in \mathbb{Y}$, the well group theory [12] studies the robustness of the homology of the pre-image of a , $f^{-1}(a)$ with respect to perturbations of the mapping f . Roughly speaking, the homology of a topological space \mathbb{X} , $H_*(\mathbb{X})$, measures its topological features, where the rank of the 0-, 1- and 2-dimensional homology groups corresponds to the number of connected components, tunnels, and voids, respectively. Let a be a point in \mathbb{Y} , and let $B_a(r)$ be a ball of radius r surrounding a . Let h be an r -perturbation of f (under some metric). The inclusion map between subspaces $h^{-1}(a) \rightarrow f^{-1}(B_a(r))$ induces a linear map $i_h : H_*(h^{-1}(a)) \rightarrow H_*(f^{-1}(B_a(r)))$ between their homology groups. The *well group* $W_a(r)$ is defined as $W_a(r) = \bigcap_h \text{image } i_h$, whose elements belong to the image of each i_h for all r -perturbation h of f . Intuitively, its elements are *stable* under r -perturbations of the map.

When $a = 0$, $\mathbb{X} = \mathbb{Y} = \mathbb{R}^2$, $f^{-1}(0)$ are the critical points of vector fields on the plane. Chazal et al. [6] showed that in the case of vector fields, the well group could be computed from the *merge tree* of the magnitude of a vector field (i.e., $f_0 = \|f\|_2$, which is a scalar function). We use the correspondences between critical points and the elements in the well groups to assign robustness values to the critical points. The merge tree of f_0 is constructed by tracking the connected components of its sublevel sets $f^{-1}(-\infty, r]$ together with their degree information as they appear and merge by increasing r from 0. Each leaf node in the tree is assigned the degree of its corresponding critical point (a saddle has a degree of -1 , and a source/sink has a degree of $+1$). Each internal node has a degree the sum of its subtree. The robustness of a critical point is the height of its lowest degree zero ancestor in the merge tree, see Wang et al. [29] for details.

4 Theoretical Results

We extend the definition of robustness by considering every point as a critical point. Formally, let $x_0 \in \mathbb{R}^2$ be an arbitrary point in a vector field $v : \mathbb{R}^2 \rightarrow \mathbb{R}^2$ and $R(x_0)$ be its robustness in the vector field v_{x_0} , which is associated with the frame of reference of x_0 . We define the *extended robustness* $R : \mathbb{R}^2 \rightarrow \mathbb{R}$ of the point x_0 as the robustness of the critical point $x_0 \in \mathbb{R}^2$ in the vector field v_{x_0} . For a vector field $v : \mathbb{R}^2 \rightarrow \mathbb{R}^2$, we call a point a *locally robust critical point* (LRCP) if it is a local maximum in the extended robustness field, i.e.,

$$\nabla R(x_0) = 0, \quad H_R(x_0) < 0,$$

with the vector ∇ denoting the first derivative and the Hessian matrix H_R consisting of the second partial derivatives.

The following two theorems are the key theoretical contributions of the paper.

Theorem 1 *The extended robustness is a Galilean invariant scalar field. The locally robust critical points defined above are Galilean invariant.*

Proof. We prove the theorem by showing that for the extended robustness $R : \mathbb{R}^2 \rightarrow \mathbb{R}$, we have $R'(x') = R(x)$. The extended robustness assigns a scalar to every point $x_0 \in \mathbb{R}^2$. Let $v'(x')$ differ from a vector field $v : \mathbb{R}^2 \rightarrow \mathbb{R}^2$ by the transformation $v'(x') = Av(x)$. The magnitude $\|v_{x_0}\|_2$ of the GI field v_{x_0} from (2) is GI. From $A \in SO(2)$, it follows that

$$\|v'_{x'_0}(x')\|_2 = \|Av_{x_0}(x)\|_2 = \|v_{x_0}(x)\|_2. \quad (3)$$

As a result, the merge trees of $v_{x_0}(x_0)$ and $v'_{x'_0}(x'_0)$ are isomorphic. Together with the invariance of the degree of a critical point with respect to orthogonal transformations, that the extended robustness is GI follows. Since the extrema of the scalar field are GI and the extended robustness field is GI, it follows that LRCs are GI. \square

Theorem 2 *At any point $x_0 \in \mathbb{R}^2$, suppose: (i) $v_{x_0} : \mathbb{R}^2 \rightarrow \mathbb{R}^2$ is generic and C^2 -smooth; (ii) the directional derivative of v_{x_0} is upper bounded by a constant μ ; (iii) the second (partial) derivative of v_{x_0} is upper bounded by a constant δ ; and (iv) the absolute value of the determinant of the Jacobian is at least c . Then the extended robustness at x_0 is at least $\frac{c^2}{2\mu^2\delta}$.*

Proof. For any point $x_0 \in \mathbb{R}^2$, let $f := v_{x_0} : \mathbb{R}^2 \rightarrow \mathbb{R}^2$. Genericity from assumption (i) of f implies that for the critical point x_0 of f , there exists a small neighborhood that contains only x_0 . First, we show that a lower bound on the absolute value of the determinant of the Jacobian translates into a lower bound on the magnitude of the directional derivative of f . Let J be the Jacobian at $x_0 \in \mathbb{R}^2$ and $\det(J)$ be the determinant of the Jacobian. Assumption (iv) means that $|\det(J)| \geq c$. Let λ_1 and λ_2 ($|\lambda_1| \geq |\lambda_2|$) be the eigenvalues of J . We have,

$$|\det(J)| = |\lambda_1 \lambda_2| \geq c.$$

Assumption (ii) means that the directional derivatives of f are upper bounded in any direction by μ , i.e., $\|\frac{\partial f}{\partial u}\| \leq \mu$ for all directions $u \in \mathbb{S}^2$, which implies that the absolute values of all eigenvalues are upper bounded by μ , i.e., $|\lambda_2| \leq |\lambda_1| \leq \mu$. Hence, $|\lambda_2| \geq c' = \frac{c}{\mu}$.

Now, we show that the upper bound on the second derivative implies a lower bound on robustness. We consider the direction $u \in \mathbb{S}^2$ to be along the eigenvector associated with λ_2 . At x_0 , $|f(x_0)| = 0$. Since the magnitude of the directional derivative at x_0 is lower bounded by c' and there is an upper bound on the second derivative, we can bound the neighborhood size where the directional derivative becomes 0, i.e., how far from x_0 we must go in order for $\|f\|$ to stop growing. Let y be a point on the boundary of the isolating neighborhood of x_0 , such that $d(y, x_0) = \varepsilon$.

Then the magnitude of the directional derivative is lower bounded by $c' - \varepsilon\delta$ based on assumption (iii). The change $c' - \varepsilon\delta$ is positive for all $\varepsilon \leq \frac{c'}{\delta}$. We obtain a lower bound on the magnitude of the vector field on the boundary of the ε -neighborhood at x via integration. That is, for any y on the boundary of the isolating neighborhood of x_0 ,

$$|f(y)| \geq \int_0^\varepsilon (c' - x\delta)dx = c'\varepsilon - \frac{\delta\varepsilon^2}{2}. \quad (4)$$

For $\varepsilon \leq \frac{c'}{\delta}$, $|f(\varepsilon)|$ is an increasing function in ε ; hence x_0 is the only zero in the neighborhood. To obtain a lower bound on robustness, we lower bound the magnitude of the function on the boundary of the ε -neighborhood (i.e. the neighborhood where we know that x_0 is an isolated zero). Substituting $\varepsilon = \frac{c'}{\delta} = \frac{c}{\mu\delta}$ into Eq. 4 yields the desired lower bound, i.e.,

$$|f(y)| \geq c'\varepsilon - \frac{\delta\varepsilon^2}{2} = \frac{c^2}{\mu^2\delta} - \frac{\delta c^2}{2\mu^2\delta^2} = \frac{c^2}{2\mu^2\delta}. \quad \square$$

5 Visualization Results

We demonstrate visually that the extended robustness helps to interpret the Jacobian-based GIVF analysis. In particular, the extrema of the determinant of the Jacobian (the Jacobian-based GICPs) often coincide with the local maxima of the extended robustness (the LRCs).

Case study I: an analytic vector field. For the first case study illustrated in Fig. 2, we use an analytic vector field in (f) which contains four standard flow features, sink (a), center (b), saddle (c) and spiral source (d); each showing a different common velocity profile overlaid with a shear flow (e) that makes it impossible to view all the flow features simultaneously. As illustrated, the GIVF based on the determinant of the Jacobian (g) simultaneously highlights the Jacobian-based GICPs, which correspond to the standard flow features described in (a)-(d). On the other hand, these flow features in (g) coincide with the features surrounding the LRCs of the GIVF based on the extended robustness in (h).

Case study II: a sequence of double gyre. We use a formula describing a double gyre vector field [3] with parameters $A = 0.25$, $\omega = 1/10$, and an extended domain $[0, 6] \times [0, 1]$. Such a dataset is smooth and requires no topological simplification (see Section 5.1). As shown in Fig. 3(a), one vortex is visible at position (3, 0.5) within the standard frame of reference, and the Jacobian-based GIVF highlights two vortices within the same region in Fig. 3(b), as shown previously [3]. These Jacobian-based critical points coincide with the LRCs obtained via extended robustness in Fig. 3(c). The separators from the robustness-based GIVF coincide with the separators from the standard frame of reference, but those from the Jacobian-based GIVF do not. This observation gives an indication that the two

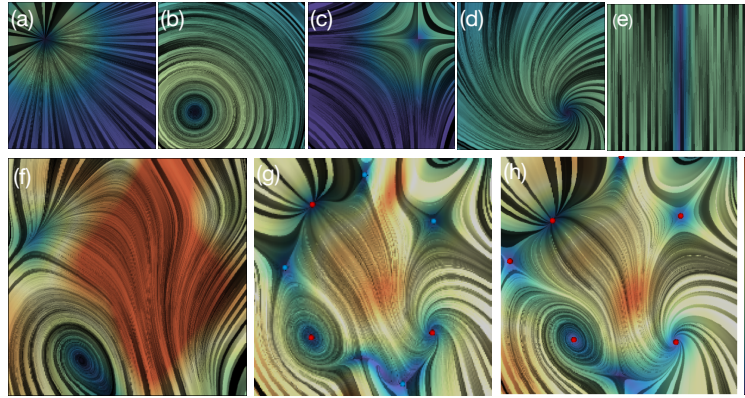


Fig. 2 Visualization of an analytic data set (f), which is created by superimposing five analytic fields (a)-(e). The colormap encodes the speed of the flow. For comparison, (g) shows the corresponding Galilean invariant vector field introduced by Bujack et al. and constructed from the extrema of the determinant of the Jacobian. The Galilean invariant critical points are marked with red nodes for vortices/sinks/sources and with blue nodes for saddles. Image courtesy of Bujack et al. [2]. (h) The Galilean invariant vector field introduced in this paper is constructed from the extended robustness. The local maxima of the extended robustness field are marked with red nodes.

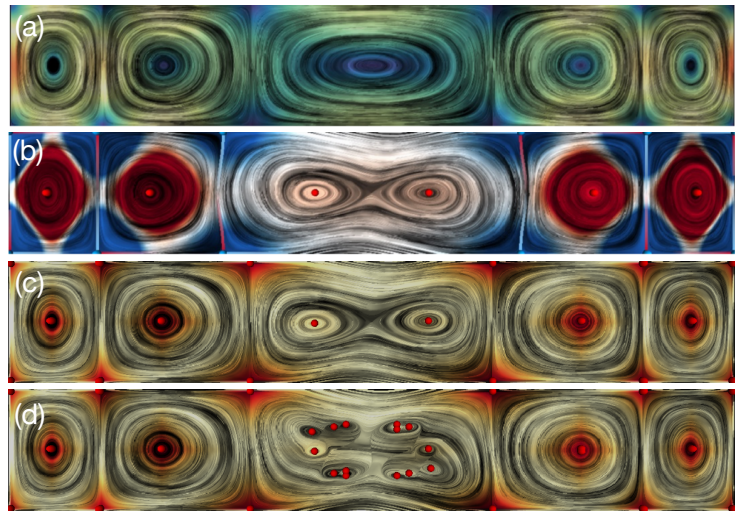


Fig. 3 Visualization of a sequence of double gyre. (a) The original flow; the colormap encodes the speed of the flow. (b) Jacobian-based Galilean invariant vector field with highlighted critical points; the flow is color-coded by the value of the determinant. (c) Robustness-based Galilean invariant vector field with highlighted critical points; the flow is color-coded by extended robustness values. (d) Robustness-based Galilean invariant vector field without contour tree pruning.

vortices detected by both robustness-based and Jacobian-based GIVF are likely true features, whereas the separators detected by the Jacobian-based GIVF are not (therefore partially addressing an open question in [3]). Furthermore, we illustrate the robustness-based GIVFs in Fig. 3(d) without topological simplification (see Section 5.1 for details).

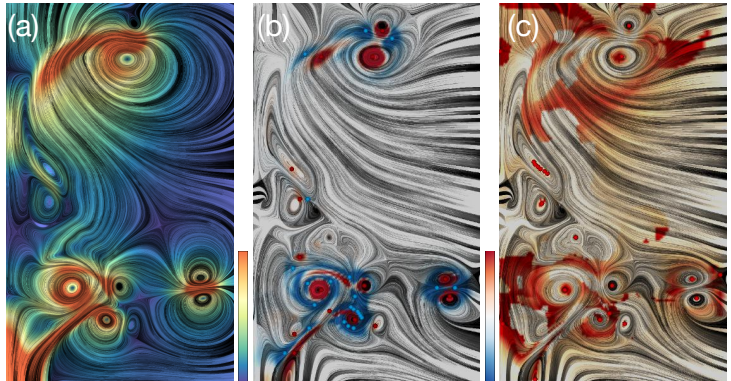


Fig. 4 Visualization of the swirling jet entering a fluid at rest. (a) The original flow; the colormap encodes the speed of the flow. (b) Jacobian-based Galilean invariant vector field with highlighted critical points; the flow is color-coded by the value of the determinant. (c) Robustness-based Galilean invariant vector field with highlighted locally robust critical points; the flow is color-coded by extended robustness values.

Case study III: swirly jet. Our last case study, illustrated in Fig. 4, focuses on a flow simulation of a swirling jet entering a fluid at rest. Such a dataset has been previously studied in the work of Bujack et al. [2]. We demonstrate visually an interpretation of its corresponding Jacobian-based GIVF with the extended robustness. As shown in Fig. 4(c), some but not all of the LRCPs are shown to coincide with the critical points extracted from Jacobian-based GIVF in Fig. 4(b). Such a discrepancy could be due to numerical issues in computing extended robustness, discretization resolution and the noisy, non-smooth data domain. How to choose the optimal parameters for topological simplification (as discussed in Section 5.1), remains an open question for both Jacobian-based and robustness-based GIVFs.

5.1 Topological Simplification

In our case studies, the extended robustness fields are often noisy, resulting in many insignificant local maxima. Analogously to Bujack et al. [2], we make use of the topological simplification tools for scalar fields to reduce the number of

local maxima to the significant ones. For an introduction to scalar topological simplification, we recommend the work of Carr et al. and Heine et al. [4, 5, 16].

For a scalar field, a contour is a connected component of a level set, which is the set of points that all have the same value in the scalar field. If we increase this value, contours can be created at local minima, join or split at saddles, and be destroyed at local maxima of the scalar field. The contour tree is an abstraction of the scalar field that is formed from shrinking each contour to a node in the tree, where each branch starts and ends at an extremum or a saddle and corresponds to a connected component in the domain. Each branch of the contour tree comes with three popular measures: persistence, volume, and hypervolume [5, 16]. Persistence is the maximal difference of the scalar values of the components of a branch, the volume is the integral over its affiliated points, and the hypervolume is the integral over the scalar values. These measures can be used to simplify the contour tree by pruning branches that do not exceed given thresholds (see Carr et al. [5]).

We compute the contour tree of the extended robustness field and prune it with respect to persistence. The result for case study I can be found in Fig. 5.

Remark. We have demonstrated that the Jacobian-based GICPs in some smooth, synthetic cases coincide with the LRCPs, whereas in noisy, real-world datasets, unambiguous equivalence among these points is difficult to find due to the resolution of the data and the different range of scalar values for topological simplification. In addition, we conjecture that the determinant of Jacobian could be considered as a first-order approximation that captures the stabilities of critical points, whereas the extended robustness captures higher order information; therefore the LRCPs do not always coincide with the Jacobian-based GICPs.

The best way to select the pruning parameters for simultaneous visualization of robust critical points in different regions of the data, remains an open question. We currently use an exploratory process to choose pruning parameters so that the LRCPs are at a level comparable to the Jacobian-based GICPs.

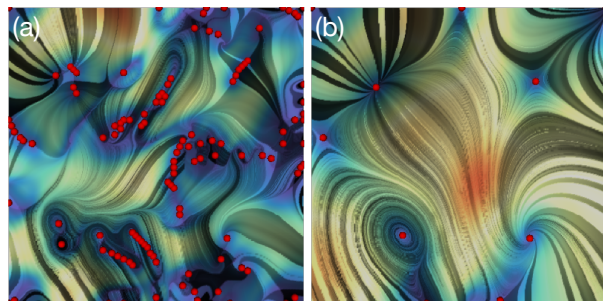


Fig. 5 Topological simplification of case study I, where the colormap encodes the speed of the flow. The robustness-based Galilean invariant vector fields before (a) and after (b) simplification are illustrated, where the locations of extended robustness local maxima are marked in red.

6 Discussion

Robustness and Jacobian. The Jacobian carries important information about the local behavior of a vector field, while robustness quantifies their global stability. In this work, we demonstrate their relations theoretically and visually. Furthermore, our results inspire discussions regarding different quantifiers of stable features within the vector field data.

Extended robustness: degeneracies and continuity. In our current framework, some critical points do not have any cancellation partner and so have large robustness values beyond the range of the maximum vector norm in the domain. This can cause boundary effects in our visualization as some critical points are detected on the boundary. Furthermore, robustness computation also assumes that each critical point is isolated within its local neighborhood. Our datasets, however, contain regions with degenerate critical points where such isolation conditions are violated (i.e., regions where the determinant of Jacobian switches sign). For the purpose of visualization, such degeneracies are handled separately.

Small changes to the vector field may introduce partner switches in the merge tree, which lead to some discontinuities in the current computation of extended robustness (see Fig. 4(c)). However this does not impact our visualization results significantly. Ensuring the continuity of the extended robustness remains an open question.

Other perturbation metrics for robustness. The robustness framework also allows a certain flexibility in defining perturbation metrics, in the sense that the L_∞ metric defined in Section 3 could be replaced by other metrics such as the L_2 metric, which incorporates both the magnitude of the vectors and the area to capture a quantity closer to the energy of a perturbation. We will investigate the effect of different perturbation metrics on the computation of extended robustness and its connection with the determinant of the Jacobian.

References

1. Bhatia, H., Pascucci, V., Kirby, R.M., Bremer, P.: Extracting features from time-dependent vector fields using internal reference frames. *Computer Graphics Forum* **33**(3), 21–30 (2014)
2. Bujack, R., Hlawitschka, M., Joy, K.I.: Topology-inspired Galilean invariant vector field analysis. *IEEE Pacific Visualization Symposium* pp. 72–79 (2016)
3. Bujack, R., Joy, K.I.: Lagrangian representations of flow fields with parameter curves. *IEEE Symposium on Large Data Analysis and Visualization* pp. 41–48 (2015)
4. Carr, H., Snoeyink, J., Axen, U.: Computing contour trees in all dimensions. *Computational Geometry* **24**(2), 75–94 (2003)
5. Carr, H., Snoeyink, J., van de Panne, M.: Simplifying flexible isosurfaces using local geometric measures. *IEEE Visualization* pp. 497–504 (2004)
6. Chazal, F., Patel, A., Skraba, P.: Computing well diagrams for vector fields on \mathbb{R}^n . *Applied Mathematics Letters* **25**(11), 1725–1728 (2012)

7. Chen, G., Palke, D., Lin, Z., Yeh, H., Vincent, P., Laramée, R.S., Zhang, E.: Asymmetric tensor field visualization for surfaces. *IEEE Transactions on Visualization and Computer Graphics* **17**(12), 1979–1988 (2011)
8. Chong, M.S., Perry, A.E., Cantwell, B.J.: A general classification of three-dimensional flow fields. *Physics of Fluids A* **2**(5), 765–777 (1990)
9. Ebling, J., Wiebel, A., Garth, C., Scheuermann, G.: Topology based flow analysis and superposition effects. In: H. Hauser, H. Hagen, H. Theisel (eds.) *Topology-based Methods in Visualization. Mathematics and Visualization.*, pp. 91–103. Springer (2007)
10. Edelsbrunner, H., Letscher, D., Zomorodian, A.J.: Topological persistence and simplification. *Discrete & Computational Geometry* **28**, 511–533 (2002)
11. Edelsbrunner, H., Morozov, D., Patel, A.: The stability of the apparent contour of an orientable 2-manifold. In: V.P. an dXavier Tricoche, H. Hagen, J. Tierny (eds.) *Topological Methods in Data Analysis and Visualization. Mathematics and Visualization.*, pp. 27–42. Springer (2010)
12. Edelsbrunner, H., Morozov, D., Patel, A.: Quantifying transversality by measuring the robustness of intersections. *Foundations of Computational Mathematics* **11**, 345–361 (2011)
13. Fuchs, R., Kemmler, J., Schindler, B., Waser, J., Sadlo, F., Hauser, H., Peikert, R.: Toward a Lagrangian Vector Field Topology. *Computer Graphics Forum* **29**(3), 1163–1172 (2010)
14. Günther, T., Schulze, M., Theisel, H.: Rotation invariant vortices for flow visualization. *IEEE Transactions on Visualization and Computer Graphics* **22**(1), 817–826 (2016)
15. Haller, G.: An objective definition of a vortex. *Journal of Fluid Mechanics* **525**, 1–26 (2005)
16. Heine, C., Schneider, D., Carr, H., Scheuermann, G.: Drawing contour trees in the plane. *IEEE Transactions on Visualization and Computer Graphics* **17**(11), 1599–1611 (2011)
17. Hunt, J.C.R.: Vorticity and vortex dynamics in complex turbulent flows. *Transactions of the Canadian Society for Mechanical Engineering* **11**(1), 21–35 (1987)
18. Jeong, J., Hussain, F.: On the identification of a vortex. *Journal of Fluid Mechanics* **285**, 69–94 (1995)
19. Kasten, J., Reininghaus, J., Hotz, I., Hege, H.C.: Two-dimensional time-dependent vortex regions based on the acceleration magnitude. *IEEE Transactions on Visualization and Computer Graphics* **17**(12), 2080–2087 (2011)
20. Lugt, H.J.: The dilemma of defining a vortex. In: U. Müller, K.G. Roesner, B. Schmidt (eds.) *Recent Developments in Theoretical and Experimental Fluids Mechanics*, pp. 309–321. Springer (1979)
21. Perry, A.E., Chong, M.S.: Topology of flow pattern in vortex motions and turbulence. *Applied Scientific Research* **53**(3-4), 357–374 (1994)
22. Pobitzer, A., Peikert, R., Fuchs, R., Schindler, B., Kuhn, A., Theisel, H., Matkovic, K., Hauser, H.: The state of the art in topology-based visualization of unsteady flow. *Computer Graphics Forum* **30**(6), 1789–1811 (2011)
23. Sahner, J., Weinkauff, T., Hege, H.C.: Galilean invariant extraction and iconic representation of vortex core lines. *IEEE VGTC Symposium on Visualization* pp. 151–160 (2005)
24. Skraba, P., Rosen, P., Wang, B., Chen, G., Bhatia, H., Pascucci, V.: Critical point cancellation in 3D vector fields: Robustness and discussion. *IEEE Transactions on Visualization and Computer Graphics* **22**(6), 1683–1693 (2016)
25. Skraba, P., Wang, B.: Interpreting feature tracking through the lens of robustness. In: P.T. Bremer, I. Hotz, V. Pascucci, R. Peikert (eds.) *Topological Methods in Data Analysis and Visualization III. Mathematics and Visualization.*, pp. 19–38. Springer (2014)
26. Skraba, P., Wang, B., Chen, G., Rosen, P.: 2D vector field simplification based on robustness. *IEEE Pacific Visualization Symposium* pp. 49–56 (2014)
27. Skraba, P., Wang, B., Chen, G., Rosen, P.: Robustness-based simplification of 2D steady and unsteady vector fields. *IEEE Transactions on Visualization and Computer Graphics* **21**(8), 930–944 (2015)
28. Song, Y.: A note on Galilean invariants in semi-relativistic electromagnetism. *arXiv:1304.6804* (2013)
29. Wang, B., Rosen, P., Skraba, P., Bhatia, H., Pascucci, V.: Visualizing robustness of critical points for 2D time-varying vector fields. *Computer Graphics Forum* pp. 221–230 (2013)
30. Wiebel, A., Garth, C., Scheuermann, G.: Localized flow analysis of 2D and 3D vector fields. *IEEE VGTC Symposium on Visualization* pp. 143–150 (2005)